Entanglement purification of hypergraph states

Lina Vandré and Otfried Gühne

Naturwissenschaftlich-Technische Fakultät, Universität Siegen, Walter-Flex-Straße 3, 57068 Siegen, Germany

Entanglement purification describes a primitive in quantum information processing, where several copies of noisy quantum states are distilled into a few copies of nearly pure states of high quality via local operations and classical communication. Especially in the multiparticle case, the task of entanglement purification is complicated, as many inequivalent forms of pure state entanglement exist and purification protocols need to be tailored for different target states. In this paper we present optimized protocols for the purification of hypergraph states, which form a family of multiqubit states that are relevant from several perspectives. We start by reformulating an existing purification protocol in a graphical language. This allows for systematical optimization and we present improvements in three directions. First, one can optimize the sequences of the protocol with respect to the ordering of the parties. Second, one can use adaptive schemes, where the measurement results obtained within the protocol are used to modify the protocols. Finally, one can improve the protocol with respect to the efficiency, requiring fewer copies of noisy states to reach a certain target state.

I. INTRODUCTION

For many tasks in quantum information processing one needs high-fidelity entangled states, but in practice most states are noisy. Purification protocols address this problem and provide a method to transform a certain number of copies of a noisy state into a single copy with high fidelity. The first protocols to purify Bell states were introduced by Bennett *et al.* [1,2] and Deutsch *et al.* [3]. The concept was then further developed for different entangled states, especially in the multiparticle setting. This includes protocols for the purification of different kinds of states, such as graph states [4,5] or *W* states [6] (see [7] for an overview). There are several examples for experimental realizations of purification protocols [8–11].

When analyzing multiparticle entanglement, the exponentially increasing dimension of the Hilbert space renders the discussion of arbitrary states difficult. It is therefore a natural strategy to consider specific families of states which enable a simple description. Graph states [12] and hypergraph states [13–15] form such families of multiqubit quantum states, as they can be described by a graphical formalism. Besides this, they found applications in various contexts, including quantum error correction [16,17], measurement-based quantum computation [18,19], Bell nonlocality [20–22], and state verification and self-testing [23,24]. Consequently, their entanglement properties were studied in various works [25,26]. Note that hypergraph states are a special case of the so-called locally maximally entangled states [13].

Concerning entanglement purification, the only known purification protocol which is valid for hypergraph states is formulated for locally maximally entangleable (LME) states by Carle *et al.* [27]. In this paper we first ask how this protocol can be translated to the hypergraph formalism. Based on this, we can then systematically develop improvements of the protocol.

Our paper is organized as follows. In Sec. II we introduce our notation and review hypergraph states. We also recall how operations like CNOT gates and Pauli operators act graphically. In Sec. III we reformulate the Carle–Kraus–Dür–de Vicente (CKDdV) purification protocol in a graphical manner, providing a different language to understand it. Based on this, we propose systematic extensions in Sec. IV, which naturally arise from the graphical formalism. We first propose two approaches to make the protocol applicable to noisy states where the original CKDdV protocol fails. Later we propose a method requiring fewer copies of noisy states to reach a certain target state. In Sec. V we extend the protocol to more qubits. We summarize in Sec. VI.

II. HYPERGRAPH STATES

In this section we present a short introduction to the class of hypergraph states and the description of transformations between them. Readers familiar with the topic may skip to the next section.

A. Definition of hypergraph states

A hypergraph $H = (V, E)$ is a set V of vertices and hyperedges $e \in E$ connecting them. Contrary to a normal graph, the edges in a hypergraph may connect more than two vertices; examples of hypergraphs are given in Fig. 1.

Hypergraph states are multiqubit quantum states, where the vertices and hyperedges of the hypergraph $H = (V, E)$ represent qubits and entangling gates, respectively. The state $|H\rangle$, corresponding to a hypergraph $H = (V, E)$, is defined as

$$|H\rangle = \prod_{e \in E} C_e |+\rangle^{\otimes|V|} \equiv U_{\mathrm{ph}} |+\rangle^{\otimes|V|}, \tag{1}$$

where C_e is a generalized controlled-Z gate, acting on qubits in the edge e as $C_e = \mathbb{1}_e - 2|11\cdots1\rangle\langle11\cdots1|_e$. If an edge
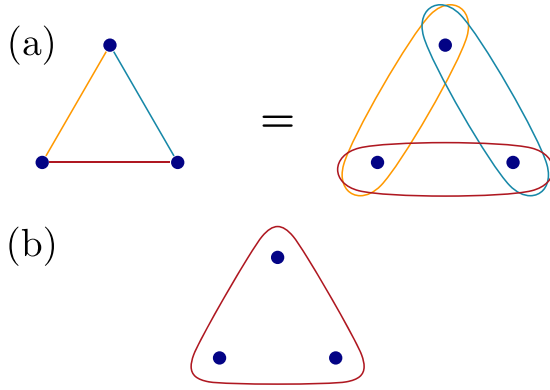
(a)

(b)

FIG. 1. Examples of graphs and hypergraphs. (a) Fully connected graph, which corresponds to the three-qubit GHZ state. In the hypergraph state formalism one often draws edges by circles (right) instead of lines as in the graph state formalism (left). (b) The hypergraph state corresponding to the hypergraph is local unitary equivalent to the state $|H\rangle = (|000\rangle + |001\rangle + |010\rangle + |111\rangle)/2$.

contains only a single vertex $|e| = 1$, then C_e reduces to the Pauli Z operator, and for two-vertex edges C_e is just the standard two-qubit controlled-phase gate. A detailed discussion of hypergraph state properties can be found in Refs. [25,28].

Similarly as for graph states, there is an alternative definition using so-called stabilizing operators. First, one can define for each vertex i a stabilizer operator

$$S_i = U_{\text{ph}} X_i U_{\text{ph}}^\dagger, \qquad (2)$$

where X_i denotes the first Pauli matrix acting on the ith qubit and U_{ph} denotes the collection of phase gates as in Eq. (1). Note that here only the gates with $i \in e$ matter. The stabilizing operators are nonlocal Hermitian observables with eigenvalues ± 1; they commute and generate an Abelian group, the so-called stabilizer.

Then a hypergraph state may be defined as a common eigenvector of all stabilizing operators S_i. Here one has to fix the eigenvalues of the S_i. Often, the state defined in Eq. (1) is called $|H_{00\cdots0}\rangle$, as it is a common eigenstate of the S_i with eigenvalue $+1$. By applying Pauli Z gates on the state, one obtains states orthogonal to $|H_{00\cdots0}\rangle$, where some of the eigenvalues are flipped to -1. By applying all possible combinations of Z gates, one obtains a basis $\{|H_\mathbf{k}\rangle = Z^\mathbf{k}|H_\mathbf{0}\rangle\}$, where $\mathbf{k}$ is a binary multi-index and $Z^\mathbf{k} = \bigotimes_{v \in V} Z_v^{k_v}$. In this notation, it holds that $S_i|H_\mathbf{k}\rangle = (-1)^{k_i}|H_\mathbf{k}\rangle$. Hence, $|H_\mathbf{k}\rangle$ is an eigenstate of S_i with eigenvalue $(-1)^{k_i}$. It is convenient to write arbitrary states in the hypergraph basis

$$\rho = \sum_{\mathbf{k}, \mathbf{k}'} c_{\mathbf{k}, \mathbf{k}'} |H_\mathbf{k}\rangle\langle H_{\mathbf{k}'}|. \qquad (3)$$

Later we will purify states in this form to the state $|H_\mathbf{0}\rangle$.

B. Operations on hypergraph states

Many operations on hypergraph states can be represented in a graphical manner. In the following, we explain the effect of applying Pauli gates X and Z, measuring in the corresponding basis σ_x and σ_z, discuss how to represent the CNOT gate graphically [29], and introduce the reduction operator P_{v_1, v_2}
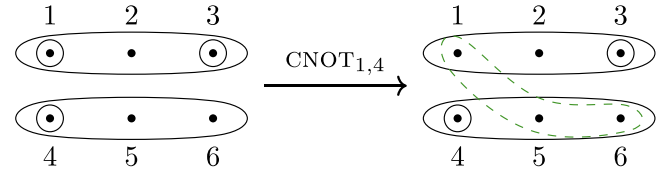

FIG. 2. Example of a CNOT$_{1,4}$ gate (with control qubit 1 and target qubit 4) performed on a hypergraph state. Shown on the left is a hypergraph with vertex set $V = \{1, \dots, 6\}$ and edge set $E = \{\{1\}, \{1, 2, 3\}, \{3\}, \{4\}, \{4, 5, 6\}\}$ and on the right the hypergraph after applying the CNOT$_{1,4}$ gate. A new edge $\{1, 5, 6\}$ appears while the edge $\{1\}$ vanishes. The effect of applying the CNOT$_{1,4}$ gate is to introduce or delete edges from the set $E_4 = \{\{1\}, \{1, 5, 6\}\}$. The underlying rule is the following [29]: One takes the so-called adjacency $\mathcal{A}(4)$ of the target qubit $t = 4$, where one first considers all edges that contain t but then removes t from it. Here we have $\mathcal{A}(4) = \{\{\}, \{5, 6\}\}$. Then E_4 contains all edges which are unions of edges from $\mathcal{A}(4)$ and the edge $\{1\}$ of the control qubit $c = 1$.

which we will need later. Note that, in the following, for Pauli matrices we use X and Z to denote the corresponding unitary transformations and σ_x and σ_z to denote the measurements. We only discuss transformations that are needed in the present paper; an overview of other transformations can be found in Ref. [28].

We have already mentioned the action of the unitary transformation Z_v on some qubit v. It adds the edge $e = \{v\}$ to the set of edges E, if it was not contained before, or removes it otherwise. For example, applying Z_2 and Z_3 to the left hypergraph state in Fig. 2 would add a circle at vertex 2 and remove the one at vertex 3.

The unitary transformation X_v on a vertex v of a hypergraph state $|H\rangle$ corresponding to the hypergraph $H = (V, E)$ is given by

$$X_v|H\rangle = \prod_{e \in E} C_e \prod_{e' \in \mathcal{A}(v)} C_{e'} |+\rangle^{\otimes |V|}, \qquad (4)$$

where $\mathcal{A}(v)$ is the adjacency of vertex v. This is a set of edges defined as

$$\mathcal{A}(v) = \{e \setminus \{v\} \mid e \in E \text{ with } v \in e\}. \qquad (5)$$

In words, to build the adjacency $\mathcal{A}(v)$ one first takes the set of edges that contain v and then removes v from them. Examples of local transformations X are given in Fig. 3.

Let us discuss now the graphical description of some local measurements on hypergraph states. In order to derive the postmeasurement state after measuring vertex v, we can
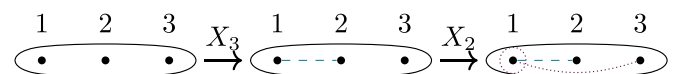

FIG. 3. Application of X operators on qubits 3 and 2. We first apply X_3 on the left graph. The adjacency of qubit 3 is given by $\mathcal{A}(3) = \{\{1, 2\}\}$. This new edge is shown by the blue dashed line in the middle graph. We then apply X_2 to the middle graph. The adjacency of qubit 2 is given by $\mathcal{A}(2) = \{\{1\}, \{1, 3\}\}$. These new edges are shown by the purple dotted lines in the right graph.
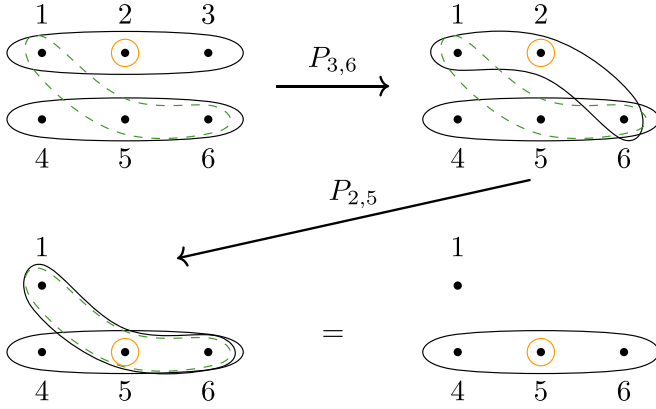
FIG. 4. Application of the reduction projectors $P_{3,6}$ and $P_{2,5}$. The projector merges two vertices and its corresponding edges to one. In the first step, we merge vertices 3 and 6. In the second step we merge vertices 2 and 5. This results in two times the same edge, the green dashed edge $\{1, 5, 6\}$ and the edge which was initially $\{1, 2, 3\}$, and such double edges cancel out.

expand the state $|H\rangle$ at this vertex as

$$|H\rangle = \frac{1}{\sqrt{2}}\left(|0\rangle_v|H_0\rangle \pm \frac{1}{\sqrt{2}}|1\rangle_v|H_1\rangle\right), \qquad (6)$$

where $|H_0\rangle$ and $|H_1\rangle$ are new hypergraph states with vertex set $V_0 = V_1 = V \setminus v$ and edge sets $E_0 = \{e \in E \mid v \notin e\}$ and $E_1 = E_0 \cup \mathcal{A}(v)$ [28]. After measuring σ_z, we therefore get either the state $|H_0\rangle$ or the state $|H_1\rangle$. Measuring σ_x leads to a superposition of these two states and often the postmeasurement state is then not a hypergraph state anymore. In our case, we only measure σ_x on qubits which are separated from other parts of the system, that is, where $|H_0\rangle = |H_1\rangle$.

Applying a CNOT_{ct} gate on a hypergraph state H, where c is the control and t the target, introduces or deletes hyperedges of the set $E_t = \{e_t \cup c \mid e_t \in \mathcal{A}(t)\}$. The new edge set after applying the CNOT_{ct} gate is given by

$$E' = E \triangle E_t, \qquad (7)$$

where $A \triangle B = A \cup B \setminus A \cap B$ is the symmetric difference of two sets. Since $C_e^2 = \mathbb{1}$, double edges cancel out. Therefore, the CNOT_{ct} operation deletes edges which are in E and E_t and introduces edges which are only in E_t. For example, in the left part of Fig. 2, the neighborhood of vertex 4 is given by $N(4) = \{\{\}, \{5, 6\}\}$ and therefore $E_4 = \{\{1\}, \{1, 5, 6\}\}$.

Finally, another operator which will be important later is the reduction operator P_{v_1, v_2}, which maps two qubits to a single qubit. In the computational basis, the reduction operator is written as

$$P_{v_1, v_2} = |0\rangle\langle 00| + |1\rangle\langle 11|. \qquad (8)$$

It merges two vertices v_1 and v_2 into one, which we call v_2. This action changes edges which contain v_1 into edges which contain v_2 and deletes edges e and e', with $e \neq e'$ but $(e \setminus \{v_1\}) = (e' \setminus \{v_2\})$. The new edge set will therefore be

$$E' = (\{e \in E | v_1 \notin e\} \triangle \{f \cup \{v_2\} | f \in \mathcal{A}(v_1)\}). \qquad (9)$$

An example is shown in Fig. 4.

III. THE CKDDV PURIFICATION PROTOCOL

In this section we discuss the only known protocol which works for hypergraph states [27]; we will refer to it as the CK-DdV protocol. Originally, it was formulated for more general LME states. We first reformulate the purification protocol in a graphical manner, which makes it intuitively understandable. Based on this reformulation, we can then propose improvements.

In the simplest case, the aim is to purify a three-qubit state ρ to a pure hypergraph state, chosen to be the state $|H_0\rangle = C_{\{123\}}|+\rangle^{\otimes 3}$. The state is distributed between three parties, Alice, Bob, and Charlie. In the following, we explicitly describe the subprotocol which reduces noise on Alice's qubit. There are equivalent subprotocols on Bob's and Charlie's qubits. The protocol is performed on two copies of a state ρ. Alice holds qubit a_1 of the first state and qubit a_2 of the second state, and equivalently for Bob and Charlie.

The key idea of the protocol is to induce a transformation on the basis elements of the form

$$|H_{i,j,k}\rangle|H_{i',j',k'}\rangle \rightarrow \delta_{i,i'}|H_{i,j+j',k+k'}\rangle, \qquad (9)$$

where $\delta_{i,i'}$ denotes the Kronecker delta. This means that the subprotocol compares the indices i and i' on Alice's qubits and the state is discarded when $i \neq i'$. This map drives a general state as in Eq. (3) closer to the desired hypergraph state. In detail, the subprotocol which implements this transition is given by the following protocol.

Protocol 1 (CKDdV protocol).

(0) Alice, Bob, and Charlie share two copies of a state.

(i) Alice applies a local CNOT_{a_1, a_2} gate on her qubits.

(ii) Bob and Charlie apply local reduction operators P_{v_1, v_2} on their qubits.

(iii) Alice measures qubits a_1 in the σ_x basis. She keeps the state if the outcome is $+1$ and discards it otherwise.

In Fig. 5 it is shown how the basis elements $|H_{000}\rangle|H_{i00}\rangle$ transform.

In order to purify the full state, one needs to choose a sequence of subprotocols in which these subprotocols are applied on different parties. In Ref. [27], the sequence ABC-CAB-BCA was favored, as it seems to perform better than just repeating the sequence ABC. The reason is that the qubit of Charlie becomes more noisy due to the backaction from the subprotocols purifying Alice's and Bob's qubits.

IV. IMPROVING PROTOCOL PERFORMANCE

In order to purify towards one state of a certain fidelity, one needs a number of input states, which depends exponentially on the number of iterations, as in each run of the protocol a certain fraction of states is discarded. Therefore, it is of high interest to apply the subprotocols in a sequence which works as efficiently as possible. As already pointed out by Carle et al. [27], it depends on the input state whose sequence is the most advantageous and it is not trivial to see which sequence is optimal. Carle et al. decided to use the sequence $S = \text{ABC-CAB-BCA}$ in all their applications, since it performs well in many cases. In the following, we will ask whether the proposed sequence really is the best and how we can potentially find better sequences.
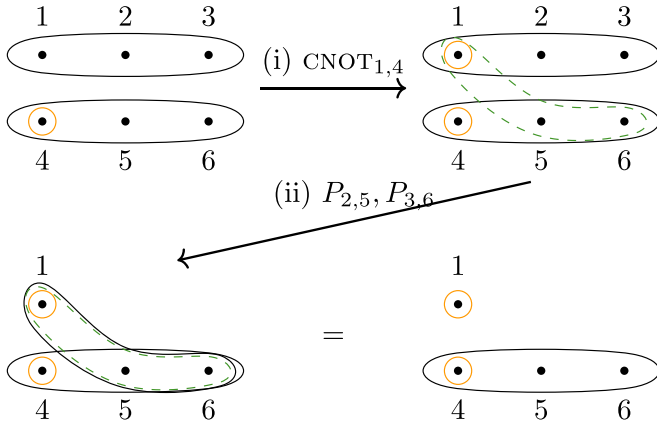
FIG. 5. The CKDdV protocol, as described in Protocol 1. The transformation of the two basis elements $|H_{000}\rangle|H_{100}\rangle$ is shown. In step (i) Alice performs a local CNOT$_{1,4}$ gate. Then Bob and Charlie apply local reduction operators $P_{2,5}$ and $P_{3,6}$, respectively. Double edges cancel out, so the green dashed line and the former edge {1, 2, 3} vanish. In step (iii) Alice measures qubit 1 in the σ_x basis. If there is a single-qubit edge on vertex 1, such as the orange one in this figure, her measurement outcome will be -1 and therefore the state gets discarded. If one ignores all orange single-qubit edges in the figure, this corresponds to the transformation of the basis elements $|H_{000}\rangle|H_{000}\rangle$. In this case, Alice's measurement outcome will be $+1$ and the remaining state $|H_{000}\rangle$ is kept.

One should notice that in step (ii) of the protocol a large fraction of states is discarded. The operator P_{v_1,v_2} corresponds to a positive map which maps two qubits that are in the same state to one qubit and both qubits are discarded if they are in different states. This can be seen as one outcome of a measurement. In Sec. IV B we will ask whether one can reduce the number of discarded states.

A. Improved and adaptive sequences

Consider a noisy three-qubit state $\rho(p)$, where p is a noise parameter for some noise model which should be purified to the pure hypergraph state $|H_{000}\rangle\langle H_{000}|$. Clearly, for a fixed sequence S there is a maximal amount of noise until which the state can still be purified and there is a regime where one cannot purify it anymore.

Interestingly, for some parameter regimes where the state cannot be purified, the purification protocol does not converge towards a state with random noise but towards a specific state which is a mixture of two states: $\frac{1}{2}(|H_{000}\rangle\langle H_{000}| + |H_{001}\rangle\langle H_{001}|)$, $\frac{1}{2}(|H_{000}\rangle\langle H_{000}| + |H_{010}\rangle\langle H_{010}|)$, or $\frac{1}{2}(|H_{000}\rangle\langle H_{000}| + |H_{100}\rangle\langle H_{100}|)$. This observation gives insight into how good the purification works on different parties. The protocol eliminates noise on two parties but fails on the third party. For example, if we apply the sequence $S = \text{ABC}$, in the cases we tested, there is a regime where the state does not get purified but converges to $\frac{1}{2}(|H_{000}\rangle\langle H_{000}| + |H_{001}\rangle\langle H_{001}|)$.

This is consistent with the explanation given in Ref. [27] that the purification has a disadvantage on Charlie's site. It may be explained as follows. By performing the protocol at one party, one aims to reduce noise on this party. As an

unwanted side effect, one increases noise on the other parties. This happens because if there is noise on the first input state, the local reduction operator will "copy" it to the second state [see Eq. (9)]. So when choosing the sequence $S = \text{ABC}$, one increases the noise on Charlie's qubit two times before purifying it the first time.

How well the protocol performs on each party can be analyzed using the measurement statistics obtained in step (iii) of the protocol. The probability to measure outcome $+1$ in step (iii) on a qubit belonging to a certain party give insight into how much noise the state on this party has. On the perfect target state, one does not detect any noise and therefore measures outcome $+1$ with probability equal to one. If one applies the protocol to the state $\frac{1}{2}(|H_{000}\rangle\langle H_{000}| + |H_{001}\rangle\langle H_{001}|)$, however, one obtains outcome $+1$ with a probability equal to one or 0.5, depending on which subprotocol was applied. If it was the subprotocol where Alice's or Bob's qubits are measured in step (iii), the probability is equal to one. If it was the subprotocol where Charlie's qubit was measured, the probability is 0.5. So, by evaluating the probabilities to measure outcome $+1$ in step (iii) of the protocol, one can analyze the efficiency of the sequence.

All in all, we use two approaches to find better sequences. The first approach is to find an optimal sequence which allows a high noise tolerance and will be applied later without further observation of the statistics. The second approach uses two sequences where we switch from one to the other depending on the measurement outcomes during the process. The first approach helps to find sequences which are more efficient also for purification of states with a low noise level. The second approach gives a method to purify states which would not be purifiable otherwise.

We assume that we know how often we want to apply the protocol and therefore how many copies of the initial state are needed. We perform the first subprotocol on all copies and get a certain fraction of output states. We then perform the second subprotocol on all output states and so on. With this procedure, we do multiple measurements on copies of states such that we can approximate a probability from the frequency of a certain outcome. We further assume that we repeat this procedure several times, that is, we produce a certain number of copies of input states, purify them, and start again from the beginning. In each run, we can vary the sequence, using what we have learned in the run before. We restrict ourselves to sequences of length 9. The best sequence we find in this way we call S_1.

It is not known how the efficiency of the sequence depends on the state. Therefore, even if the state is known, one needs to sample which sequence works best. However, there are some observations which can be used to find better sequences. We notice that it is reasonable to consider permutations of A, B, and C together. We further notice that the first party of the triple experiences the largest impact. It is also a good strategy to address the same party in two consecutive rounds, that is, on the last position of one triple and on the first position of the following triple. The sequence proposed by Carle *et al.* fulfills all mentioned properties and is in principle a good starting sequence. After gaining experience in how efficient the sequence works for the given state, one can exchange a few positions and evaluate its impact. In Tables I and IV we

TABLE I. Sequences S_1 and S_2, approximate weight vectors $\vec{a}$, and bounds b for states with three kinds of noise. For further explanation see the text.

Parameter	$\mathcal{E}_{\mathrm{WN}}(\rho, p)$	$\mathcal{E}_{\mathrm{deph}}(\rho, p)$	$\mathcal{E}_{\mathrm{depo}}(\rho, p)$
S_1	ABC-CBA-ABC	ABC-CBA-CBA	ABC-CAB-BCA
S_2	BAB-CAB-ABA	CCC-ACB-CBC	BBB-BCB-BBB-BAB
$\vec{a}$	(0.33,0.35,0.32)	(0.35,0.43,0.21)	(0.35, 0.34, 0.31)
b	0.35	0.39	0.44

see that the optimal sequences S_1 we found for different states support our observations. Every triple is a permutation of A, B, and C. We see that except for one case, the first position of one triple is equal to either the first or the last position of the previous triple. However, it consumes many states to find good sequences. Another strategy could be to estimate the corresponding density matrix of the given state by local tomography and find the optimal sequence by simulations on the computer.

With the second approach, we give a way to purify states which cannot be purified by sequence S_1 because their initial fidelity is slightly beyond the threshold. We start using sequence S_1 and switch to sequence S_2 depending on the measurement outcomes of step (iii). Our switching condition is the following: After each measurement of step (iii), we evaluate the probability to measure -1 for the given party. Based on the last three probabilities associated with the same party, we make a decision to switch or not. For $\vec{x}$ the vector of these three probabilities, where x_3 is the newest probability, we switch, if the product of the vectors $\vec{a}\vec{x}$ exceeds a bound b where $\vec{a}$ is a weight vector. In real applications we cannot evaluate the probability. We suggest to count appearance of certain outcomes and estimate the probability from the frequency.

To see the efficiency of our methods, we consider different noise models. We analyze the influence of global white noise described by the channel

$$\mathcal{E}_{\mathrm{WN}}(\rho, p) = p\rho + \frac{1-p}{2^n}\mathbb{1}, \qquad (10)$$

where n is the number of qubits. In this section, the number of states is $n = 3$. We further analyze local noise channels given by $\mathcal{E}(\rho, p) = \bigotimes_{i=1}^n \mathcal{E}^i(\rho, p)$, where $\mathcal{E}^i$ is either the dephasing channel

$$\mathcal{E}_{\mathrm{deph}}^i(\rho, p) = p\rho + \frac{1-p}{2}(\rho + Z_i\rho Z_i) \qquad (11)$$

or the depolarizing channel

$$\mathcal{E}_{\mathrm{depo}}^i(\rho, p) = p\rho + \frac{1-p}{4}(\rho + X_i\rho X_i + Y_i\rho Y_i + Z_i\rho Z_i). \qquad (12)$$

The sequences, weight vectors, and bounds we found to be optimal are given in Table I. To compare the approaches, we give the noise thresholds found in Ref. [27], obtained by our sequence S_1, and obtained by the adaptive approach in Table II. The sequences we found are also better in other perspectives. If we apply the new sequences S_1 nine rounds on given input states, we see that the output states have a higher

TABLE II. Noise thresholds $p_{\min}$ reproduced from Ref. [27], gained from our sequences S_1 (see Table I), and for the adaptive approach. In the case of $\mathcal{E}_{\mathrm{depo}}(\rho, p)$ we found that the sequence from Ref. [27] was already the best sequence of length 9. Therefore, there is no improvement of $p_{\min}$ in this case.

Parameter	$p_{\min}$ from [27]	$p_{\min}$ from S_1	$p_{\min}$ from adaptive protocol
$\mathcal{E}_{\mathrm{WN}}(\rho, p)$	0.6007	0.5878	0.5876
$\mathcal{E}_{\mathrm{deph}}(\rho, p)$	0.8013	0.7803	0.7747
$\mathcal{E}_{\mathrm{depo}}(\rho, p)$	0.8136	0.8136	0.8132

fidelity than after purifying the same state nine rounds using the sequence given in Ref. [27].

B. Recycling discarded states

If one wishes to purify a state using the CKDdV protocol one needs a high number of input states in order to obtain one state of a certain fidelity. Let us count how many states we need to have one state after applying the protocol once. In step (0) of the protocol, one takes two input states. One does not lose states by applying the CNOT gate in step (i). By applying the reduction operator P_{v_1,v_2}, approximately $\frac{1}{2}$ of the pairs are lost. Since this operator is applied on two parties in step (ii), one needs approximately four pairs. In step (iii), one measures outcome $+1$ with a probability less than or equal to 1. This probability depends on the fidelity of the states and increases with increasing fidelity. So, in total, approximately eight input states are required to obtain one output state. To prepare a state for which we need to apply the protocol m times, we need more than 8^m input states. To purify, for example, a state of initial fidelity 0.93 to a state of fidelity of 0.994, we need three steps. The required number of input states to obtain one output state is roughly $8.7^3 \approx 660$. If we want to purify the same state to a fidelity of 0.999, which we reach after six steps, we need about $8.38^6 \approx 346\,000$ input states to get one new state.

It is natural to try to use the available quantum states more efficiently. In step (ii) of the CKDdV protocol, we perform a projective measurement and consider only one outcome, namely, P_{v_1,v_2}, which we get with probability approximately $\frac{1}{2}$. We suggest to use the states which were discarded because we measured something different than P_{v_1,v_2}. The second reduction operator $P_{v_1,v_2}^{\perp}$ is perpendicular to P_{v_1,v_2} and defined as

$$P_{v_1,v_2}^{\perp} = |0\rangle\langle 10| + |1\rangle\langle 01| = P_{v_1,v_2}(X_{v_1} \otimes \mathbb{1}_{v_2}). \qquad (13)$$

As P_{v_1,v_2}, the operator $P_{v_1,v_2}^{\perp}$ is a positive map. It maps two qubits, which are in different states, to one qubit. This can be seen as a different measurement outcome than P_{v_1,v_2}, or one may interpret the set $\{P_{v_1,v_2}, P_{v_1,v_2}^{\perp}\}$ as a quantum instrument.

In the original CKDdV protocol one keeps the state only after measuring $P_{b_1,b_2}P_{c_1,c_2}$. There are three more possible measurement outcomes: $P_{b_1,b_2}P_{c_1,c_2}^{\perp}$, $P_{b_1,b_2}^{\perp}P_{c_1,c_2}$, and $P_{b_1,b_2}^{\perp}P_{c_1,c_2}^{\perp}$. In the cases of measuring $P_{v_1,v_2}^{\perp}$ on at least one party, one obtains a postmeasurement state on which one can apply some corrections to get a state which is similar to the input state. One can collect these states and further purify them.

TABLE III. In Protocol 2, step (iii b), Alice measures her qubit a_1 in the Z basis. If her outcome is -1, Bob and Charlie have to apply local corrections to their qubits. The local corrections depend on their measurement outcomes from step (ii) and are given in this table. The first case is shown in Fig. 6.

Measurement outcomes	Local correction	
	Bob	Charlie
$P_{b_1,b_2} P_{c_1,c_2}^\perp$	Z	$\mathbb{1}$
$P_{b_1,b_2}^\perp P_{c_1,c_2}$	$\mathbb{1}$	Z
$P_{b_1,b_2}^\perp P_{c_1,c_2}^\perp$	Z	Z

So one can write down a modified protocol of the CKDdV protocol. Here we give the subprotocol which reduces noise on Alice's qubits. The subprotocols for Bob and Charlie work equivalently.

Protocol 2 (improved CKDdV protocol).

(0) Alice, Bob, and Charlie share two copies of a state.

(i) Alice applies a local CNOT_{a_1,a_2} gate on her qubits.

(ii) Bob and Charlie perform a measurement on their qubits and measure the local reduction operators P_{v_1,v_2} and $P_{v_1,v_2}^\perp$. If the measurement outcome for Bob and Charlie is P_{v_1,v_2}, continue with step (iii a); otherwise continue with (iii b).

(iii a) After Bob and Charlie both measure P_{v_1,v_2}, Alice measures qubits a_1 in the σ_x basis. She keeps the state if the outcome is $+1$ and discards it otherwise.

(iii b) After measuring $P_{v_1,v_2}^\perp$ on at least one pair of Bob's and Charlie's qubits, Alice measures her qubit a_1 in the σ_z basis. If she measure $+1$, she keeps the state as it is. Otherwise, Bob and Charlie apply some local unitaries, which depend on the combinations of measurement outcomes in step (ii) and are given in Table III.

The key idea is that output states from step (iii b) can be collected and further purified. In the case of measuring $P_{v_1,v_2}^\perp$ on at least one party, the protocol gives us a transition

$$|H_{i,j,k}\rangle|H_{i',j',k'}\rangle \rightarrow |H_{i',j+j',k+k'}\rangle. \qquad (14)$$

The resulting state has in general a lower fidelity than the input state. This is caused by the same reason of "copying" noise, as discussed before. Since in the considered case the protocol does not reduce noise, the fidelity drops.

An example for Protocol 2 is shown in Fig. 6, where we assume the case that Bob measures $P_{2,5}$ and Charlie measures $P_{3,6}^\perp$. In this case, the local correction after measuring outcome -1 is applying a unitary Z_5 at qubit 5.

Given a certain number of input states which we want to purify to a target fidelity, we obtain more output states of the desired fidelity if we follow Protocol 2 instead of the original CKDdV protocol. The effect in the cases we tested turned out however to be small. As input states we chose the state $|H_{000}\rangle\langle H_{000}|$ mixed with white noise. We first applied Protocol 1 three times, that is, once on each party, and computed the fidelity F_3 of the output states. Then we applied Protocol 2 on the same input states and compared how many more output states of fidelity greater than or equal to F_3 we get. In Fig. 7 we show how much the number of output states increases by using Protocol 2, depending on the fidelity F_0 of the input states. In the chosen cases, we get approximately 0.4% more
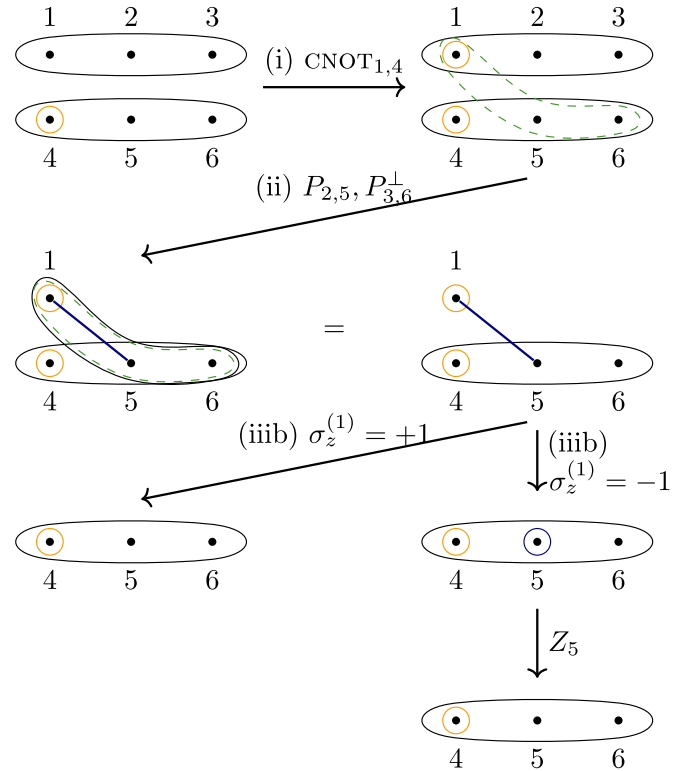

FIG. 6. Modified Protocol 2 for the same initial states as shown in Fig. 5 for the case to measure $P_{b_1,b_2} P_{c_1,c_2}^\perp$ in step (ii). Alice performs a $\sigma_z^{(1)}$ measurement on her qubit 1 of the state in the second row. If she gets outcome $+1$ in step (iii b), the resulting state is the same as the initial state (qubits 4–6). If she gets outcome -1, Bob's qubit 5 has a decoration, which he needs to correct. After Bob applies a local Z_5 unitary on qubit 5, again the resulting state is the same as the initial state (qubits 4–6). Note that this is only the case if there is no noise on qubits 2 and 3, as shown in this figure. In general, one obtains the state given in Eq. (14).
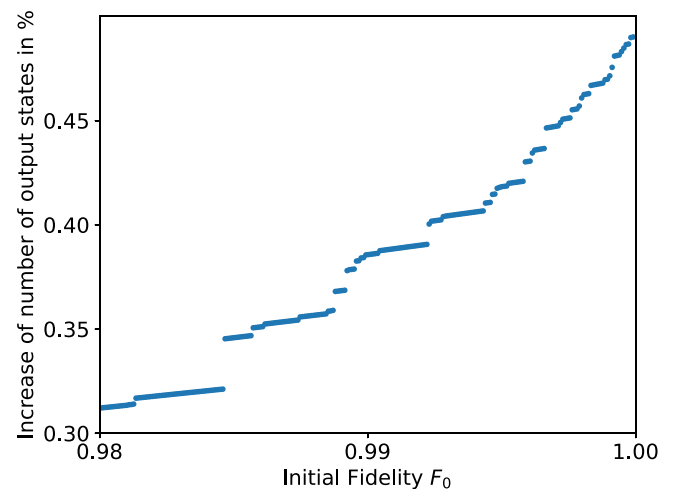

FIG. 7. Effect of using Protocol 2 instead of the original CKDdV protocol. The input states are given by $\mathcal{E}_{\text{WN}}(|H_0\rangle\langle H_0|, p)$. We first apply Protocol 1 three times and compute the fidelity F_3 of the output states. Then we apply Protocol 2 on the same input states and compare how many more output states of fidelity greater than or equal to F_3 we get. The increase of output states by using Protocol 2 is shown, depending on the fidelity F_0 of the input states.
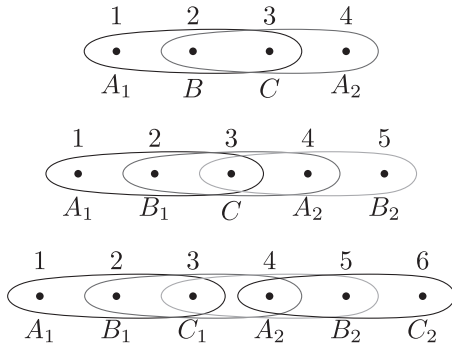
FIG. 8. Linear 3-colorable and 3-regular hypergraph states with four, five, and six qubits. The colors are denoted by A, B, and C. Note that two qubits which have the same color, for example, qubits 1 and 4, still belong to different parties. Since we are restricted to local operations, we can only perform operations on qubits of the same party, which in general is not on qubits of the same color.

output states from using Protocol 2 instead of the CKDdV protocol.

A similar idea of reusing states which get discarded in most protocols was proposed in Ref. [26]. Zhou *et al.* considered Bell states and reused states from the last step of the protocol, which is equivalent to step (iii) in the CKDdV protocol.

V. GENERALIZATION TO MORE QUBITS

The methods described here can also be applied to states with more qubits and different arrangement of edges. We restrict our attention to hypergraphs which are k-regular and k-colorable. A hypergraph is k-regular if all edges $e \in E$ have order k and it is k-colorable if it is possible to color vertices of a hypergraph using k colors such that no two vertices of the same color share a common edge. For example, the hypergraph states shown in Figs. 2 and 8 are 3-colorable and 3-regular. In this section we discuss purification protocols to hypergraph states of more than three qubits which are 3-colorable and 3-regular. In the following, we will denote the colors by A, B, and C.

The protocols can be generalized by letting all parties holding qubits of color A do what was described for Alice before. In the same way, parties holding a qubit of color B or C do what was described for Bob or Charlie, respectively. For an explicit formulation of the generalized protocol, see Ref. [27].

We analyzed linear 3-colorable states with up to six qubits under the influence of global white noise, dephasing, and depolarization. Specifically, the states to which we want to purify are $U_{123}U_{234}|+\rangle^{\otimes 4}$, $U_{123}U_{234}U_{345}|+\rangle^{\otimes 5}$, and $U_{123}U_{234}U_{345}U_{456}|+\rangle^{\otimes 6}$, as shown in Fig. 8. We compare the noise threshold $p_{\min}$ for the sequence proposed in Ref. [27] with new sequences S_1, found using methods described in Sec. IV A.

Our results are shown in Table IV. One sees that in the case of white noise for more qubits, the differences in the noise threshold $p_{\min}$ become more significant. Therefore, especially in these cases it is more relevant to find good sequences. For the tested states with dephasing and depolarization noise, the noise threshold is constant or varies slightly, respectively.

TABLE IV. Noise thresholds $p_{\min}$ for the sequence S_{CKDdV} proposed in Ref. [27] and new sequences S_1. The index of the state gives the number of qubits. In the case of $\mathcal{E}_{\text{depo}}(\rho_3, p)$ we found that the sequence from Ref. [27] was already the best sequence of length 9. Therefore, there is no improvement of $p_{\min}$. When we found (nontrivially) different sequences of the same length, we marked them with an asterisk.

Parameter	$p_{\min}$ from S_{CKDdV}	$p_{\min}$ from S_1	Sequence S_1
$\mathcal{E}_{\text{WN}}(\rho_3, p)$	0.6007	0.5878	ABC-CBA-ABC
$\mathcal{E}_{\text{WN}}(\rho_4, p)$	0.4633	0.4396	ABC-ACB-BCA
$\mathcal{E}_{\text{WN}}(\rho_5, p)$	0.3901	0.3486	ABC-ABC-CBA
$\mathcal{E}_{\text{WN}}(\rho_6, p)$	0.3341	0.3017	ABC-ACB-BAC*
$\mathcal{E}_{\text{deph}}(\rho_3, p)$	0.8013	0.7803	ABC-CBA-CBA
$\mathcal{E}_{\text{deph}}(\rho_4, p)$	0.8014	0.7803	ABC-CBA-CBA*
$\mathcal{E}_{\text{deph}}(\rho_5, p)$	0.8014	0.7803	ABC-CBA-CBA*
$\mathcal{E}_{\text{deph}}(\rho_6, p)$	0.8014	0.7803	ABC-CBA-CBA*
$\mathcal{E}_{\text{depo}}(\rho_3, p)$	0.8137	0.8136	ABC-CAB-BCA
$\mathcal{E}_{\text{depo}}(\rho_4, p)$	0.8306	0.8122	BAC-CBA-CAB
$\mathcal{E}_{\text{depo}}(\rho_5, p)$	0.8358	0.8128	ACB-BCA-CBA
$\mathcal{E}_{\text{depo}}(\rho_6, p)$	0.8144	0.8121	ABC-CBA-CAB

VI. CONCLUSION AND OUTLOOK

In this paper we discussed protocols for entanglement purification of hypergraph states. First, we reformulated the CKDdV protocol in a graphical language. This offers an alternative way to understand the protocol and, furthermore, it allows one to search for systematic extensions. Consequently, we introduced several improvements of the original protocol. These improvements are based on different sequences, adaptive schemes, and methods to recycle some of the unused states. While these modifications are conceptually interesting and can indeed improve the performance in various examples, the amount of improvement in realistic examples seems rather modest.

The problem of finding efficient sequences is also relevant for purification protocols for other states and was raised, for example, in Ref. [4] in the context of 2-colorable graph states. The methods developed here can be applied to this case, but also to all purification protocols which follow the concept introduced by Bennett *et al.* [1].

A further open question is how the effects of our methods scale with the number of qubits. Another open question is whether Protocol 2 can be further improved so that the effect becomes more significant.

[1] C. H. Bennett, H. J. Bernstein, S. Popescu, and B. Schumacher, Phys. Rev. A **53**, 2046 (1996).

[2] C. H. Bennett, D. P. DiVincenzo, J. A. Smolin, and W. K. Wootters, Phys. Rev. A **54**, 3824 (1996).

[3] D. Deutsch, A. Ekert, R. Jozsa, C. Macchiavello, S. Popescu, and A. Sanpera, Phys. Rev. Lett. **77**, 2818 (1996).

[4] H. Aschauer, W. Dür, and H.-J. Briegel, Phys. Rev. A **71**, 012319 (2005).

[5] C. Kruszynska, A. Miyake, H. J. Briegel, and W. Dür, Phys. Rev. A **74**, 052316 (2006).

[6] A. Miyake and H. J. Briegel, Phys. Rev. Lett. **95**, 220501 (2005).

[7] W. Dür and H. J. Briegel, Rep. Prog. Phys. **70**, 1381 (2007).

[8] P. G. Kwiat, S. Barraza-Lopez, A. Stefanov, and N. Gisin, Nature (London) **409**, 1014 (2001).

[9] J.-W. Pan, S. Gasparoni, R. Ursin, G. Weihs, and A. Zeilinger, Nature (London) **423**, 417 (2003).

[10] X.-M. Hu, C.-X. Huang, Y.-B. Sheng, L. Zhou, B.-H. Liu, Y. Guo, C. Zhang, W.-B. Xing, Y.-F. Huang, C.-F. Li, and G.-C. Guo, Phys. Rev. Lett. **126**, 010503 (2021).

[11] C.-X. Huang, X.-M. Hu, B.-H. Liu, L. Zhou, Y.-B. Sheng, C.-F. Li, and G.-C. Guo, Sci. Bull. **67**, 593 (2022).

[12] M. Hein, J. Eisert, and H. J. Briegel, Phys. Rev. A **69**, 062311 (2004).

[13] C. Kruszynska and B. Kraus, Phys. Rev. A **79**, 052304 (2009).

[14] R. Qu, J. Wang, Z.-s. Li, and Y.-r. Bao, Phys. Rev. A **87**, 022311 (2013).

[15] M. Rossi, M. Huber, D. Bruß, and C. Macchiavello, New J. Phys. **15**, 113022 (2013).

[16] P. W. Shor, Phys. Rev. A **52**, R2493 (1995).

[17] T. Wagner, H. Kampermann, and D. Bruß, J. Phys. A: Math. Theor. **51**, 125302 (2018).

[18] R. Raussendorf and H. J. Briegel, Phys. Rev. Lett. **86**, 5188 (2001).

[19] M. Gachechiladze, O. Gühne, and A. Miyake, Phys. Rev. A **99**, 052304 (2019).

[20] V. Scarani, A. Acín, E. Schenck, and M. Aspelmeyer, Phys. Rev. A **71**, 042325 (2005).

[21] O. Gühne, G. Tóth, P. Hyllus, and H. J. Briegel, Phys. Rev. Lett. **95**, 120405 (2005).

[22] M. Gachechiladze, C. Budroni, and O. Gühne, Phys. Rev. Lett. **116**, 070401 (2016).

[23] T. Morimae, Y. Takeuchi, and M. Hayashi, Phys. Rev. A **96**, 062321 (2017).

[24] F. Baccari, R. Augusiak, I. Šupić, J. Tura, and A. Acín, Phys. Rev. Lett. **124**, 020402 (2020).

[25] O. Gühne, M. Cuquet, F. E. S. Steinhoff, T. Moroder, M. Rossi, D. Bruß, B. Kraus, and C. Macchiavello, J. Phys. A: Math. Theor. **47**, 335303 (2014).

[26] L. Zhou, W. Zhong, and Y.-B. Sheng, Opt. Express **28**, 2291 (2020).

[27] T. Carle, B. Kraus, W. Dür, and J. I. de Vicente, Phys. Rev. A **87**, 012328 (2013).

[28] M. Gachechiladze, Quantum hypergraph states and the theory of multiparticle entanglement, Ph.D. thesis, Universität Siegen, Fakultät IV - Naturwissenschaftlich-Technische Fakultät, 2019.

[29] M. Gachechiladze, N. Tsimakuridze, and O. Gühne, J. Phys. A: Math. Theor. **50**, 19LT01 (2017).